J. Plasma Physics (2007), *vol.* 73, *part* 2, *pp.* 231–239.
doi:10.1017/S002237780600448X First published online 19 July 2006 Printed in the United Kingdom

Spectrum analysis of plasma produced by pulsed laser ablation of GaAs

AI HUA LIU

College of Physics and Electronics, Shandong Normal University, 250014, Jinan, People's Republic of China
(iiiiiihua@yahoo.com.cn)

(Received 4 February 2006)

Abstract. A time-resolved diagnostic technique was used to investigate the emission spectra from the plasmas produced by 1.06 μm, 10 ns pulsed laser ablation of semiconductor GaAs. The characteristics of the species in plasma produced at different ambient pressure were analyzed. The full width at half maximum of the spectral line was measured and analyzed according to obtained spectra of the excited atoms; several line broadening factors were estimated according to our experimental conditions and the results indicate that the Stark broadening is the main broadening mechanism. Under the assumption of local thermodynamic equilibrium, the time evolution of electron number density was deduced from the Stark broadening measurements.

1. Introduction

Pulsed laser ablation of material has proved to be a useful technique and has been widely used in many fields such as laser treatment of surfaces, pulsed laser deposition (PLD) of thin films, mass spectrometry, and nanotechnology [1–3]. Although many studies on the interaction between lasers and solid material have been done [4–8], the different mechanisms involved in a laser ablation process, including laser absorption, expansion dynamics, condensation, ionization, and recombination, are rather complex and it is essential to perform more experiments for better understanding of the interaction between the pulsed laser and the material. In the present work, the optical emission from the plasma produced by a 1.06 μm, 10 ns Nd:YAG pulsed laser ablation of GaAs was detected and analyzed. The full width at half maximum (FWHM) of the spectral line was measured and the spectral line broadening mechanism was analyzed. The electron number density was deduced from the measured line broadening.

2. Experimental

The details of the experimental arrangement have been given in [9]. The 1.06 μm laser pulse with 10 ns pulse width produced from a Q-switched Nd:YAG laser device (Quanta Ray DCR-3) was focused onto the polished target surface by a quartz focusing lens L1 ($f = 6.3$ cm). Its maximum output energy was 1 J, and the focus spot size of the laser beam was 0.66 mm in diameter. The sample was positioned on a sample holder in a chamber pumped by a mechanical pump. The chamber and lens L1 were mounted on two two-dimensional movable plates respectively.

By adjusting synchronistically these two plates along the direction of the incident laser beam, the plasma emission spectrum was recorded as a function of the distance, d, from the target surface. In the direction perpendicular to the incident laser beam, two cylindrical lenses (L2 and L3) were used to image the plasma optical emission onto the entrance of the slit of an ISA (HR-320) spectrum analyzer with 1:1 magnification. The dispersed emission was subsequently detected by an optical multi-channel analyzer (PARC OMA III). An accurate trigger delayer that was synchronistically triggered by the electric Q-switched signal produced by the YAG laser device was used to control the delay time, at which the spectrum was recorded. Moreover, a photo diode and a digitizing oscilloscope (Tektronix TDS 620A) were used to calibrate the time delay. By changing the delay time t_{d}, one can get the time-resolved emission spectra.

3. Results and discussions

3.1. Analysis of plasma emission

Figures 1(a)–(c) show the temporal evolution of the spectra obtained in the wavelength range 395–435 nm at $d = 0.75$ mm. The laser power density is 9×10^9 W cm^{-2} and the ambient pressures are (a) 1 atm, (b) 1000 Pa and (c) 5 Pa. Figure 1(d) gives the temporal evolution of the spectra obtained under the same conditions as Fig. 1(c) except that the measuring position is $d = 1.25$ mm. The results show that an intense continuum emission is produced instantaneously after the pulse laser reaches the surface of the target and disappears at about 200 ns of delay time. As is known, the continuum is related to the strong collisions between the free electrons and the excited atoms or the ions (free–free emission, known as the bremsstrahlung) and the recombination of electrons with ions (free–bound emission) [10]. Thus it can be concluded that there must be a lot of electrons, excited atoms and ions in the ejected vapor near the surface of the irradiated target. That is to say, the plasma has been produced. Comparing Figs 1(a), (b) and (c), it can be found that the intensity of the continuous spectra increases with increasing the ambient pressure. This is because the probability of collision increases with the increase of the ambient pressure. At about 30 ns, the spectra from N^+ ions at 399.5 nm and Ga^+ ions at 425.1 nm and 426.2 nm that are superposed on the continuum emerge, these spectra also quickly disappear because of the recombination of electrons with ions. At first, the emitted species density is very high (see Sec. 3.3), ions will be impacted frequently by other species, so the line is broad. With increasing the delay time, the species density decreases and the line becomes narrower. From Figs 1(c) and (d), it is observed that the signal of the N^+ ions disappears at 5 Pa because of the reduction of the density of nitrogen atoms.

With the decrease of the intensity of continuum spectra, the intensities of the emissions from Ga atoms at 403.3 nm and 417.2 nm increase gradually and reach the respective maximum at nearly the same time and then decrease with time. The lines obtained at the pressure of 1 atm last a long time, up to 2000 ns, which is much longer than the duration of the excited state of the Ga atom. So it can be concluded that Ga atoms are generated and excited constantly during traveling to the laser source. Moreover, the lines last much longer at 1 atm than at 5 Pa. This is because at high ambient pressure, ambient air brings pressure to bear on the plasma, so the plasma flume can last a long time with high density.

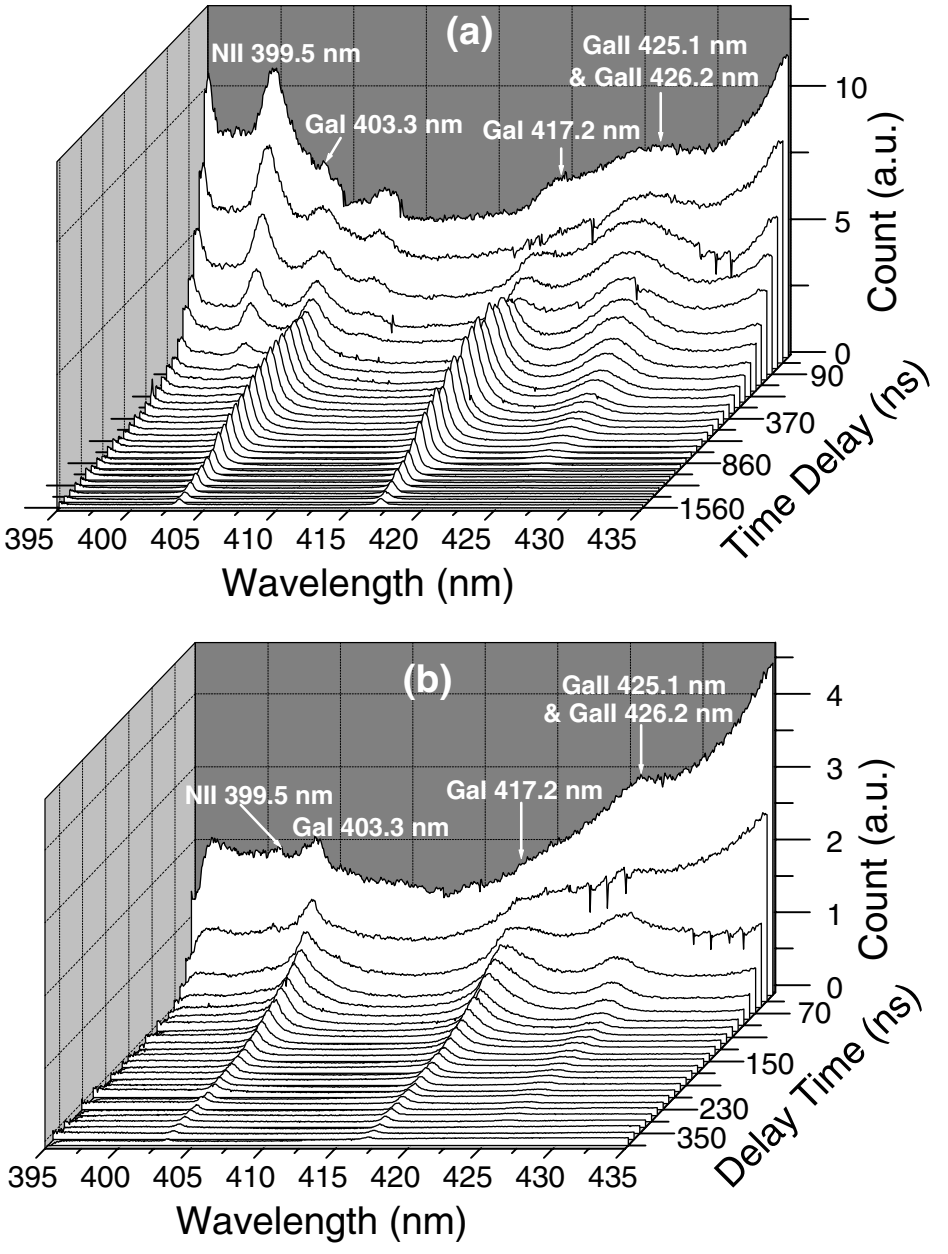

Figure 1. The temporal evolution of the spectra obtained in the wavelength range 395–435 nm at laser power density of 9×10^9 W cm^{-2}. The ambient pressures are (a) 1 atm, (b) 1000 Pa, (c) 5 Pa and (d) 5 Pa. (a)–(c) are recorded at the measuring position $d = 0.75$ mm, and (d) is at $d = 1.25$ mm.

We can also obviously find the emissions from As^+ ions at 400.6 nm and 408.4 nm in Figs 1(c) and (d), but cannot find them in Figs 1(a) and (b). The reason is that these emissions are too weak to be unshrouded by the strong continuum spectra. In addition, it can be found from Fig. 1 that the two lines from Ga^+ ions at 425.1 nm and 426.2 nm are superposed at high pressure and separated at peak position at

https://doi.org/10.1017/S002237780600448X Published online by Cambridge University Press

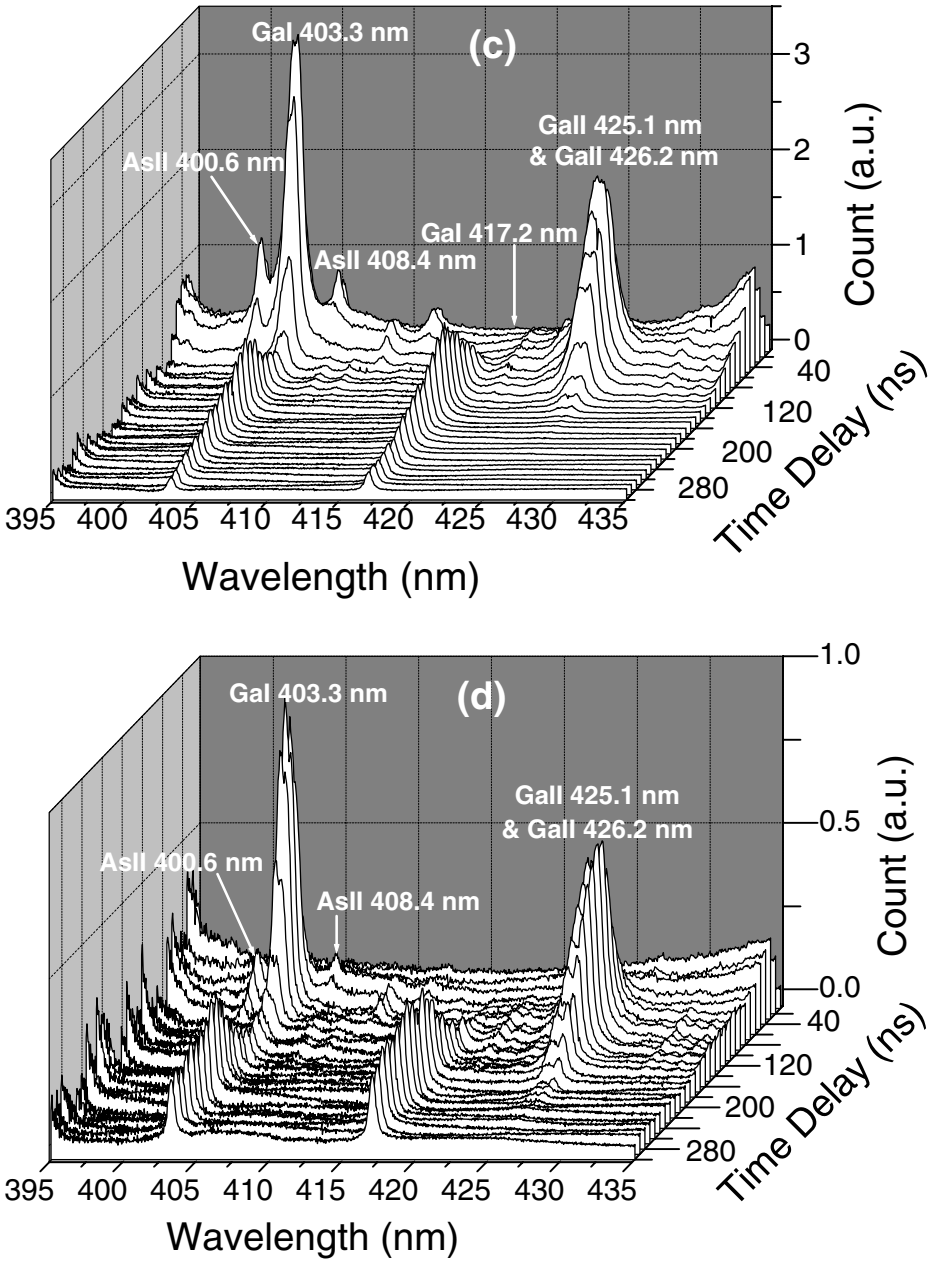

Figure 1. Continued.

low pressure. This has proved that the ambient pressure has an important effect on the line broadening (for details see Sec. 3.2).

3.2. Analysis of line broadening

The broadening of spectral lines can be described by FWHM. Figure 2 shows the FWHM of GaI 403.3 nm and GaI 417.2 nm obtained at $d = 0.75$ mm. The

https://doi.org/10.1017/S002237780600448X Published online by Cambridge University Press

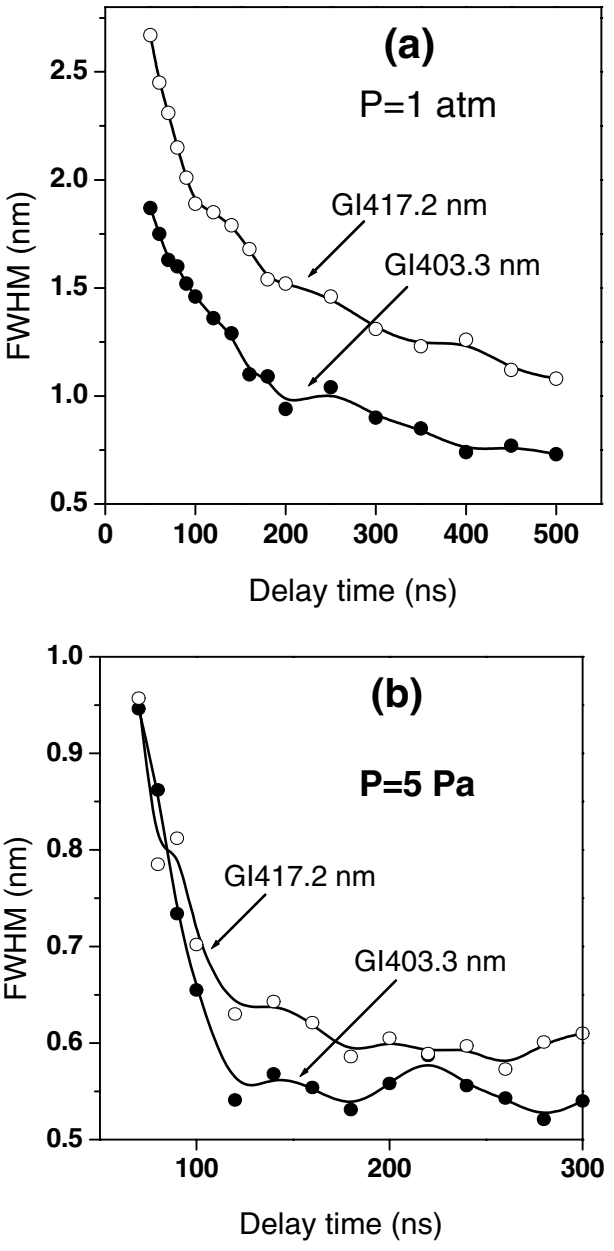

Figure 2. The measured FWHM of emission lines from the Ga atom at 403.3 nm and 417.2 nm at 0.75 mm from the target surface. The corresponding ambient pressures are (a) 1 atm and (b) 5 Pa.

corresponding laser power density is 9×10^9 W cm^{-2} and the ambient pressure is (a) 1 atm and (b) 5 Pa. The results show that, at the initial stage of plasma generation at a pressure of 1 atm, the FWHM is as great as 26 Å and decreases quickly with increasing delay time. Comparing Figs 2(a) and (b), one can find that the FWHM of the spectrum obtained at 5 Pa is smaller than that at 1 atm. Moreover, the time at which the FWHM decreases to a steady value is shorter at 5 Pa.

https://doi.org/10.1017/S002237780600448X Published online by Cambridge University Press

Line broadening is a complicated function of the environment of the radiating atoms and ions. There are several possible mechanisms of line broadening in plasmas: natural, Doppler, pressure (includes Stark), self-absorption and instrumental broadening etc. The ultimate profile of every line is a sum of all possible profiles. In general, there are only one or two is the main broadening process.

The natural linewidth can be evaluated by using Heisenberg's uncertainty principle. Both lower and upper transition levels contribute to the linewidth yielding the total uncertainty. The half width is given by the sum of the spontaneous transition probabilities of all lines originating from the two levels. That is

$$\Delta\lambda_{ik} = \frac{\lambda_{ik}^2}{2\pi c}\left(\sum_m A_{mi} + \sum_n A_{nk}\right) \tag{1}$$

where i, k correspond to the upper and lower levels of transition with the wavelength λ_{ik}, A_{mi}, A_{nk} are transition probabilities of all lines originating from the two levels and c is the velocity of light. According to formula (1), the natural linewidth for Ga emission at 403.3 nm is the order of magnitude of 10^{-5} nm. This value is several orders of magnitude less than those we got in our experiment. So the natural linewidth for this emission can be neglected completely.

The Doppler effect is caused by thermal motion of the radiator, which shortens or lengthens the frequency of the photon emitted. The broadening caused by the Doppler effect can be expressed as

$$w = 2\sqrt{\ln 2}\sqrt{2kT\lambda_0^2/mc^2} \tag{2}$$

where k is Boltzmann's constant, c the velocity of light, m the mass of the particle, λ_0 the wavelength of the line, and T the temperature of the plasma; the electron temperature is used here and can be estimated by relative line intensity measurement [9]. Using (2), we get Doppler broadening the order of magnitude of 10^{-2} nm. This value is also much smaller compared with the measured linewidth obtained in the experiment although it is much greater than the calculated natural linewidth above. So the Doppler broadening is not the main line broadening mechanism.

Self-absorption broadening refers to a phenomenon in which omitted photons are reabsorbed partly during their passage through the plasma. As the absorption profile is of the same shape as the emission profile, the largest reabsorption occurs at the center of the line or central wavelength. The actual line profile is changed as a result of the lowering of the maximum intensity accompanied by a corresponding increase in apparent FWHM. Strong self-absorbed spectral lines emitted from a homogeneous plasma are characterized by a plateau in the line center [11]; we did not find any plateau phenomena for all the spectral lines. Thus, the self-absorption broadening can be ignored.

As for the instrumental broadening, in our experiment, the dispersion of the grating on the exit slit is about 1 nm mm^{-1} and with matched entrance and exit slits of 25 μm, so the instrumental linewidth is only 0.025 nm.

Thus, according to the analysis above, the possible main mechanism of line broadening is only pressure broadening. Pressure broadening includes the effects of collisions with neutral particles (van der Waals broadening), resonance interactions between identical particles (resonance broadening), and collisions with charged particles (Stark broadening). The first two factors are important only in weakly ionized plasmas. For highly ionized, high-density plasmas, the last is most important,

the strong electric field resulting from charged particles producing a broadening of the transitions between the split atomic levels. The broadening associated with these micro electric fields is essentially the Stark broadening. So we have a conclusion that the broadening of the spectrum lines of GaI at 403.3 nm and 417.2 nm in our experiment is mainly attributed to the Stark broadening.

At low ambient pressure, because of the quick expansion of the plasma, Stark broadening decreases quickly with time, and measured FWHM is smaller compared with that at higher pressure. This is why the two spectrum lines of GaI at 403.3 nm and 417.2 nm measured above are superposed completely at a pressure of 1 atm and separated partly at a pressure of 5 Pa.

3.3. Electron density

Since the Stark broadening is the dominant line broadening mechanism, using the assumption of local thermodynamic equilibrium (LTE), we can estimate the number density of the electrons in the plasma by measuring the linewidth of the individual line. The FWHM of a Stark broadening line $\Delta\lambda_{1/2}$ is related to the electron density N_e [10]

$$\Delta\lambda_{1/2} = 2W\left(\frac{N_e}{10^{16}}\right) + 3.5A\left(\frac{N_e}{10^{16}}\right)^{1/4}\left[1 - \frac{3}{4}N_D^{-1/3}\right]W\left(\frac{N_e}{10^{16}}\right). \quad (3)$$

The first term in (3) gives the contribution from electron broadening, and the second term is the ion broadening correction; W is the electron impact parameter, A is the ionic impact broadening parameter, and N_D is the number of particles in the Debye sphere and is given by [11]

$$N_D = 1.72 \times 10^9 \frac{[T(eV)]^{3/2}}{[N_e(cm^{-3})]^{1/2}}, \quad (4)$$

where T is the electron temperature in eV. Using (3) and (4) and the measured Stark broadening data, the electron density can be calculated. W and A are weak functions of temperature; we can use the values of W and A for $T = 10\,000$ K in the calculation (data can be obtained from [12]). In our measurement, because we are short of data for the parameters W and A of the Ga atom, the N II 399.5 nm line was used to estimate the electron density. However, we can only give the data in the early 200 ns region because of the short lifetime of N^+ ions. The obtained results are shown in Fig. 3; it can be seen that the electron density at the initial stage is very high and decreases swiftly with time during the early stage of expansion of the plasma. In fact, because the ionic contribution is typically much smaller [13] owing to the weaker dependence on the ion density [14], it can be neglected in a typical pulsed laser induced plasma. Thus only the first term in (3) remains, meaning that the electron density is approximately proportional to the FWHM of Stark broadening. So the measured FWHM of the emission line in Fig. 2 gives the evolution of electron density. It can be seen that the electron density continues to decrease with time after 200 ns and then reaches a relatively steady value after about 1000 ns and 300 ns for 1 atm and 5 Pa, respectively.

4. Conclusions

A time-resolved diagnostic technique was used to investigate the emission spectra from the plasmas produced by 1.06 μm, 10 ns pulsed laser ablation of the

https://doi.org/10.1017/S002237780600448X Published online by Cambridge University Press

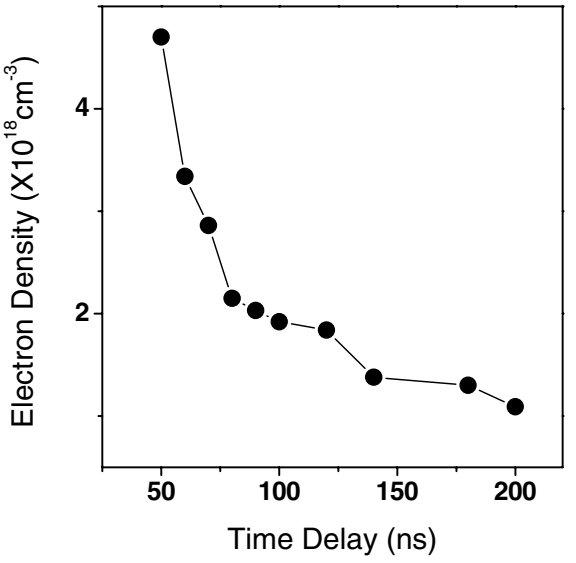

Figure 3. The electron density of plasma obtained at the pressure of 1 atm and the distance of 0.75 mm from the target surface.

semiconductor GaAs. The characteristics of the plasma and line broadening mechanism were analyzed. The results show that the ambient pressure has an important effect on the properties of plasmas such as intensity, emission lifetime and line broadening. In our experiment, Stark broadening is the main broadening mechanism. The electron number density deduced from the Stark broadening measurements shows that the electron density is very high and decreases swiftly with increasing delay time at the initial stage of the plasma expansion and then decreases slowly to a relatively steady value after about 1000 ns and 300 ns for 1 atm and 5 Pa, respectively.

Acknowledgements

The author is grateful for the financial support of the National Natural Science Foundation of China (10474059) and the Provincial Natural Science Foundation of Shandong (Y2003A01), P.R. China.

References

[1] Chrisey, D. B. and Hubler, C. K. 1994 *Pulsed Laser Deposition of Thin Films*. New York: Wiley.

[2] Forgarassy, E. and Lazare, S. 1992 *Laser Ablation of Electronic Materials: Basic Mechanisms and Applications*. Amsterdam: Elsevier Science.

[3] Zhigilei, L. V. and Dongare, A. M. 2002 Multiscale modeling of laser ablation: Applications to nanotechnology. *Comput. Model. Eng. Sci*. **3**, 539–555.

[4] Mazhukin, V. I., Nossov, V. V., Smurov, I. and Flamant, G. 2004 Modelling of radiation transfer in low temperature nanosecond laser-induced plasma of Al vapour. *J. Phys. D: Appl. Phys*. **37**, 185–199.

[5] Claeyssens, F., Henley, S. J. and Ashfolda, M. N. R. 2003 Comparison of the ablation plumes arising from ArF laser ablation of graphite, silicon, copper and aluminium in vacuum. *J. Appl. Phys*. **94**, 2203–2211.

[6] Man, B. Y., Wang, X. T. and Liu, A. H. 1998 Transport of plasmas produced by pulsed laser ablation of HgCdTe. *J. Appl. Phys.* **83**, 3509–3513.

[7] Harilal, S. S., Bindhu, C. V., Tillack, M. S., Najmabadi, F. and Gaeris, A. C. 2003 Internal structure and expansion dynamics of laser ablation plumes into ambient gases. *J. Appl. Phys.* **93**, 2380–2388.

[8] Zeng, X. Z., Mao, X. L., Wen, S. B., Greif, R. and Russo, R. E. 2004 Energy deposition and shock wave propagation during pulsed laser ablation in fused silica cavities. *J. Phys. D: Appl. Phys.* **37**, 1132–1136.

[9] Man, B. Y. 1998 Particle velocity, electron temperature, and density profiles of pulsed laser-induced plasmas in air at different ambient pressures. *Appl. Phys. B* **67**, 241–245.

[10] Gefeki, G. 1976 *Principles of Laser Plasmas*. New York: Wiley Interscience, pp. 549, 593.

[11] Hermann, J., Boulmer-Leborgne, C. and Hong, D. 1998 Diagnostics of early phase of an ultraviolet laser induced plasma spectral lines analysis considering self-absorption. *J. Appl. Phys.* **83**(2), 691–696.

[12] Griem, H. R. 1964 *Plasma Spectroscopy*. New York: McGraw-Hill, p. 463.

[13] Tamby, R., Singh, R. and Thareja, R. K. 1992 Studies on recombining Al-plasma using 1.06, 0.532, 0.355, and 0.266 μm laser radiation. *J. Appl. Phys.* **72**, 1197–1199.

[14] Griem, H. R. 1968 Semiempirical formulas for the electron-impact widths and shifts of isolated ion lines in plasmas. *Phys. Rev.* **165**, 258–266.